π-Bonded Disulfur. Structure of Disulfurbis(bis(diphenylphosphino)ethane)iridium(I) Chloride · Acetonitrile[1]

Wesley D. Bonds, Jr., and James A. Ibers*

Contribution from the Department of Chemistry, Northwestern University, Evanston, Illinois 60201. *Received September 23, 1971*

Abstract: The structure of disulfurbis(bis(diphenylphosphino)ethane)iridium(I) chloride·acetonitrile, $[Ir(S_2)((C_6H_5)_2PCH_2CH_2P(C_6H_5)_2)_2]Cl \cdot CH_3CN$, has been determined from three-dimensional X-ray data collected by counter methods. This compound crystallizes in space group D_{2d}^4-$P\bar{4}2_1c$ of the tetragonal system with four formula weights per cell (a = 22.064 (9), c = 20.747 (9) Å). The observed and calculated densities are 1.51 (2) and 1.486 g/cm^3, respectively. Full-matrix least-squares refinement of the structure has yielded a final conventional R factor of 0.050 (on F) for the 3041 independent reflections with $F^2 > 3\sigma(F^2)$. The ions and solvate molecule occupy general positions in the cell. The $[Ir(S_2)((C_6H_5)_2PCH_2CH_2P(C_6H_5)_2)_2]^+$ cation displays approximately trigonal-bipyramidal coordination and is nearly isostructural with the previously reported oxygen carriers, $[M(O_2)((C_6H_5)_2PCH_2CH_2P(C_6H_5)_2)_2]^+$ (M = Ir, Rh). The disulfur molecule is π bonded at an equatorial site, with an average Ir–S distance of 2.41 (2) Å. The four phosphorus atoms complete the coordination sphere at 2.33–2.37 Å from the metal. While the S–S linkage of 2.066 (6) Å is similar to that reported for octasulfur (2.060 (3) Å), it is significantly longer than the 1.889-Å S–S bond in free disulfur. The Ir–S_2 bonding is easily rationalized in terms of the π-bonding model previously advanced for the d^8 oxygen carriers.

Complexation of diatomic molecules to transition metal ions is a subject of continuing biochemical interest. In particular, a systematic structural investigation encompassing the $[IrX(O_2)(CO)(P(C_6H_5)_3)_2]$ (X = Cl,[2] I[3]) and $[M(O_2)(dppe)_2]^+$ (M = Ir, Rh)[4-6] molecular oxygen carriers has provided meaningful correlations between the reversibility of oxygen uptake and the geometry of M–O_2 bonding. X-Ray structural determinations on these four trigonal-bipyramidal species have revealed that O_2 binds to the metal in the π-bonding fashion at an equatorial site. Furthermore, the O–O and, to a lesser extent, the M–O bond lengths are markedly affected by variations in metal dπ-electron availability as governed by the electronegativity of the metal or substituents attached to it. The $[IrI(O_2)(CO)(P(C_6H_5)_3)_2]$ complex with its long 1.509 (23)-Å O–O bond is an irreversible O_2 carrier, while $[IrCl(O_2)(CO)(P(C_6H_5)_3)_2]$ (O–O, 1.30 (3) Å) releases molecular oxygen when nitrogen is bubbled through a solution of the complex.[7] Subsequent investigations disclosed a significantly shorter 1.418 (11)-Å O–O distance in the reversible carrier, $[Rh(O_2)(dppe)_2]^+$, than in the irreversible carrier, $[Ir(O_2)(dppe)_2]^+$, where the dioxygen bond length is 1.625 (23) Å. These findings have been rationalized in terms of a π-bonding scheme[4,5] similar to that devised by Chatt[8] and Dewar[9] for the platinum–ethylene bond in Zeise's salt. As a result, the effect on oxygen uptake and oxygen geometry from changes in ligand or metal in these Ir and Rh systems is well understood, and the need for additional structural data is obviated.

The isolation of a series of niobium(III) complexes of the type $[NbX(Cp)_2(S_2)]$ (X = Cl, Br, I, SCN)[10] was the first indication that transition metals could also stabilize diatomic molecules of the heavier group VIa elements. Unlike molecular oxygen, disulfur is not prevalent at normal temperatures and pressures,[11] although molecular S_2 possesses a triplet $^3\Sigma_g^-$ ground state reminiscent of diatomic oxygen.[12] X-Ray structural analysis confirmed the presence of π-bonded disulfur and revealed the shortest (1.73 Å) known sulfur–sulfur bond.[13] Recently, Ginsberg and Lindsell[14] reported that S_8 and Se_8 fragment under relatively mild conditions to form $[Ir(L_2)(dppe)_2]^+$ (L = S, Se) and $[Rh(S_2)(dmpe)_2]^+$ when exposed to the metal–tetraphosphine complexes. Chemical evidence suggests that $[Ir(S_2)(dppe)_2]^+$ is structurally similar to the oxygen analog and indicates that the S_2 moiety is irreversibly bound to the iridium atom. Although S_2 is formally similar to O_2, the presence of low-lying d orbitals could have a pronounced effect on the mode of bonding. It thus seems important to the subject of the bonding of small molecules to transition metals generally and of oxygen specifically to establish the trends in S_2 bonding with metal and ligand. As a first step, we have undertaken a three-dimensional, X-ray structure analysis of the complex $[Ir(S_2)(dppe)_2]Cl \cdot CH_3CN$, and we report the results here.

Collection and Reduction of Intensity Data

Red-orange crystals of $[Ir(S_2)(dppe)_2]Cl \cdot CH_3CN$, prepared by the method outlined in ref 14, were generously supplied by Dr. A. P. Ginsberg.

---

(1) Presented in part at the 162nd National Meeting of the American Chemical Society, Washington, D. C., Sept 1970, INOR 156.

(2) S. J. La Placa and J. A. Ibers, *J. Amer. Chem. Soc.*, 87, 2581 (1965).

(3) J. A. McGinnety, R. J. Doedens, and J. A. Ibers, *Inorg. Chem.*, **6**, 2243 (1967).

(4) J. A. McGinnety and J. A. Ibers, *Chem. Commun.*, 235 (1968).

(5) J. A. McGinnety, N. C. Payne, and J. A. Ibers, *J. Amer. Chem. Soc.*, **91**, 6301 (1969).

(6) Abbreviations used: dppe, bis(diphenylphosphino)ethane; dmpe, bis(dimethylphosphino)ethane; Cp$^-$, cyclopentadienyl.

(7) L. Vaska, *Science*, **140**, 809 (1963).

(8) J. Chatt, *J. Chem. Soc.*, 2939 (1953).

(9) M. J. S. Dewar, *Bull. Soc. Chim. Fr.*, **18**, C71 (1951).

(10) P. M. Treichel and G. P. Werber, *J. Amer. Chem. Soc.*, **90**, 1753 (1968).

(11) F. A. Cotton and G. Wilkinson, "Advanced Inorganic Chemistry," 2nd ed, Wiley, New York, N. Y., 1966.

(12) G. Herzberg, "Molecular Spectra and Molecular Structure," Vol. I, Van Nostrand, Princeton, N. J., 1950, p 566.

(13) L. Dahl, as cited in ref 10 and 14.

(14) A. P. Ginsberg and W. E. Lindsell, *Chem. Commun.*, 232 (1971).

Anal. Calcd for $[Ir(S_2)((C_6H_5)_2PCH_2CH_2P(C_6H_5)_2)_2]Cl\cdot CH_3CN$, $C_{54}H_{51}ClNP_4S_2Ir$: C, 57.36; H, 4.60; Cl, 3.14; P, 10.97; S, 5.68. Found: C, 57.44, H, 4.75; Cl, 3.33; P, 11.21; S, 5.76.

Additional evidence in support of the monosolvate formulation is provided by quantitative pmr spectroscopy of $[Ir(S_2)(dppe)_2]Cl\cdot CH_3CN$ dissolved in deuterated solvent.[15]

Equiinclination Weissenberg and precession photography as well as optical examination confirmed that the crystals have $4/mmm$ Laue symmetry. Systematic absences ($h00$, h odd; hhl, l odd) strongly suggest that the material crystallizes in the noncentrosymmetric space group $D_{2d}{}^4$-$P\bar{4}2_1c$.[16]

Cell constants and their standard deviations were determined at 24° from a least-squares refinement[17] of the setting angles of 12 reflections centered[18] on a Picker four-circle, computer-controlled diffractometer. The iridium complex crystallizes in a unit cell of dimensions $a = 22.064$ (9), $c = 20.747$ (9) Å (λ 1.54056 Å). The density calculated for eight formula units per cell, 1.486 g/cm^3, is in tolerable agreement with the value of 1.51 (2) g/cm^3 determined by flotation in aqueous zinc chloride. Thus no crystallographic symmetry requirements need be imposed upon the ions or solvent molecule.

The prismatic crystal selected for collection of intensity data was girdled by all eight faces of the $\{110\}$ and $\{100\}$ forms and capped by the $\{001\}$, (101), and $(0\bar{1}1)$ faces. Its 0.0123-mm^3 volume was calculated, in part, from the axial dimensions 0.19 × 0.19 × 0.45 mm. In preparation for an absorption correction, these distances were measured on a microscope fitted with a micrometer eyepiece. The compound has a linear absorption coefficient of 73.8 cm^{-1} for Cu Kα radiation.[19]

The specimen was mounted on the diffractometer with the longest dimension [001] coincident with the spindle axis. In order to minimize the possibility of multiple reflections, the crystal was deliberately misaligned by approximately 6° from the original setting. Crystal mosaicity was checked by measuring ω scans through several strong reflections, employing a narrow source and an open counter.[20] The average width of a peak at half-height was 0.17°, which is acceptable.

Intensity data were collected by the θ-2θ scan technique at a scan rate of 0.5°/min. The scan range was taken $-0.85°$ from the 2θ value calculated for Kα_1 to 0.85° from the 2θ value calculated for Kα_2. Stationary-counter, stationary-crystal background counts of 20 sec were taken at each end of the scan range. Cu Kα radiation, prefiltered through 1.0-mil Ni foil, was employed. The scintillation counter positioned 32.5 cm from the crystal was provided with a 7 × 7 mm aperture; the pulse-height analyzer was set to admit about 90% of the Cu Kα peak. Copper foil attenuators were automatically inserted when the intensity of the diffracted beam exceeded about 7000 counts/sec.

A total of 3494 unique reflections ($h > k$ and $h, k, l \geq 0$) was collected in the shell extending to $\theta = 55°$. In addition, 103 Friedel pairs ($h > k \geq 0$, $\pm l$) were gathered in the range $1° \leq \theta \leq 15°$ for comparison of anomalous dispersion effects in this noncentrosymmetric space group. Intensities of three strong reflections in diverse regions of reciprocal space were monitored every 75 reflections. Their mildly irregular deviations ($<\pm2.0\%$) yielded no clear indication of crystal decomposition or electronic instability.

The data were processed as previously described.[18,21] After the background correction, the standard deviation $\sigma(I)$ of the corrected intensity I was estimated using a value of $p = 0.04$. The intensities were then corrected for Lorentz-polarization effects. Tests showed that transmission factors varied from 0.26 to 0.35, so an absorption correction was calculated.[17] Of the 3494 reflections collected, 453 had $I < 3\sigma(I)$ and were treated as unobserved. The 3041 remaining reflections were subsequently employed in the structure solution and refinement outlined below.

Structure Solution and Refinement

In the least-squares refinements,[17] the function minimized is $\Sigma w(|F_o| - |F_c|)^2$, where $|F_o|$ and $|F_c|$ are the observed and calculated structure amplitudes and w, the weighting function, is $4F_o{}^2/\sigma^2(F_o{}^2)$. The residuals R_1 and R_2 are defined as $R_1 = \Sigma||F_o| - |F_c||/\Sigma|F_o|$ and $R_2 = [\Sigma w(|F_o| - |F_c|)^2/\Sigma wF_o{}^2]^{1/2}$. The scattering factors used for the nonhydrogen atoms were calculated by Cromer and Waber;[22] hydrogen scattering factors were those calculated by Stewart, *et al.*[23] Both the real and imaginary components of the anomalous scattering factors[19] for Ir, Cl, P, and S were included in all structure factor calculations.

The iridium atom was located from a Fourier summation calculated with normalized structure factors and phased by a direct methods procedure.[17] However, attempts to locate correctly any of the other seven heavy atoms from this synthesis were unsuccessful. Based on this Ir position, successive least-squares refinements and difference Fourier maps provided positional and thermal parameters for the remaining nonhydrogen atoms. In succeeding cycles of refinement, the eight heavy atoms and the aliphatic carbon atoms were allowed to vibrate anisotropically. The eight phenyl rings were constrained as rigid groups with C–C distances set at 1.397 Å and C–C–C angles fixed at 120.0°.

The conventional and weighted residuals converged to 0.060 and 0.093 for the 3041 reflections and 206 variables. Hydrogen atom contributions were then calculated from the assumed geometry of the rings, and a tetrahedral geometry was assumed for the four aliphatic carbon atoms. In these calculations, a C–H bond distance of 0.9 Å and an isotropic thermal parameter of

---

(15) A. P. Ginsberg, private communication.

(16) "International Tables for X-ray Crystallography," Kynoch Press, Birmingham, England, 1969.

(17) In addition to local computer programs, those used in this investigation include local modifications of Coppens' DATAP absorption program, the Busing–Levy ORFFE error function program, Zalkin's FORDAP Fourier program, and the Main–Woolfson–Germain MULTAN direct methods program. Our group least-squares program, NUCLS, in its nongroup form, closely resembles the Busing–Levy ORFLS program.

(18) P. W. R. Corfield, R. J. Doedens, and J. A. Ibers, *Inorg. Chem.*, **6**, 197 (1967).

(19) D. T. Cromer and D. Libermann, *J. Chem. Phys.*, **53**, 1891 (1970).

(20) T. C. Furnas, "Single Crystal Orienter Instruction Manual," General Electric Co., Milwaukee, Wis., 1957.

(21) R. J. Doedens and J. A. Ibers, *Inorg. Chem.*, **6**, 204 (1967).

(22) D. T. Cromer and J. T. Waber, *Acta Crystallogr.*, **18**, 104 (1965).

(23) R. F. Stewart, E. R. Davidson, and W. T. Simpson, *J. Chem. Phys.*, **42**, 3175 (1965).

Table II. Final Positional and Thermal Parameters for $[Ir(S_2)((C_6H_5)_2PCH_2CH_2P(C_6H_5)_2)_2]Cl\cdot CH_3CN$

Atom	x	y	z	β_{11}[a] or B, Å^2	β_{22}	β_{33}	β_{12}	β_{13}	β_{23}
Ir	0.19694 (3)[b]	0.35533 (3)	0.22806 (4)	0.00129 (2)	0.00119 (2)	0.00157 (2)	−0.00014 (1)	−0.00007 (2)	−0.00003 (2)
S1	0.1326 (2)	0.4442 (2)	0.2319 (3)	0.0019 (1)	0.0018 (1)	0.0026 (1)	0.00007 (8)	0.0002 (1)	0.0005 (1)
S2	0.2235 (2)	0.4582 (2)	0.2502 (2)	0.0018 (1)	0.0020 (1)	0.0020 (1)	−0.00029 (9)	−0.00011 (9)	0.00000 (9)
P1	0.1705 (2)	0.3445 (2)	0.3382 (2)	0.0015 (1)	0.0016 (1)	0.0017 (1)	−0.00014 (9)	0.00001 (9)	0.0001 (1)
P2	0.2872 (2)	0.3077 (2)	0.2568 (2)	0.0012 (1)	0.0014 (1)	0.0019 (1)	0.00011 (8)	−0.00017 (9)	0.00010 (9)
P3	0.2134 (2)	0.3783 (2)	0.1182 (2)	0.0014 (1)	0.0016 (1)	0.0018 (1)	−0.00006 (8)	−0.0002 (1)	0.0001 (1)
P4	0.1457 (2)	0.2710 (2)	0.1871 (2)	0.0013 (1)	0.0014 (1)	0.0020 (1)	−0.00025 (9)	−0.0002 (1)	−0.00005 (9)
C1	0.2238 (8)	0.2891 (8)	0.3724 (8)	0.0015 (4)	0.0018 (5)	0.0017 (5)	0.0003 (4)	−0.0005 (4)	0.0002 (4)
C2	0.2881 (7)	0.3055 (9)	0.3453 (7)	0.0018 (4)	0.0027 (5)	0.0011 (4)	0.0000 (4)	−0.0007 (4)	0.0002 (4)
C3	0.1731 (8)	0.3187 (8)	0.0715 (9)	0.0024 (5)	0.0019 (5)	0.0015 (6)	−0.0007 (4)	−0.0001 (4)	0.0000 (4)
C4	0.1735 (8)	0.2610 (8)	0.1039 (8)	0.0021 (5)	0.0017 (4)	0.0017 (5)	0.0001 (4)	−0.0004 (4)	−0.0002 (4)
Cl	0.3129 (2)	0.2196 (3)	0.4838 (3)	0.0026 (1)	0.0042 (2)	0.0033 (2)	0.0006 (1)	0.0003 (1)	0.0013 (1)
C5[c]	0.0985	0.0922	0.0426	24.9 (9)					
C6	0.1491	0.1148	0.0000	13.8 (9)					
N	0.0600	0.0750	0.0750	23.1 (7)					

Group	x_c[d]	y_c	z_c	δ	ϵ	η	B_1[e]	B_2	B_3	B_4	B_5	B_6
Ring 1	0.3503 (4)	0.3804 (4)	0.0635 (4)	2.895 (10)	2.503 (8)	−2.674 (11)	3.2 (4)	4.7 (5)	7.0 (6)	6.5 (6)	6.9 (6)	4.6 (5)
Ring 2	0.1580 (4)	0.5040 (4)	0.0619 (4)	−0.983 (8)	−2.741 (8)	−2.726 (9)	3.7 (4)	4.7 (5)	6.6 (5)	5.6 (5)	4.5 (5)	4.1 (4)
Ring 3	0.4138 (3)	0.3797 (4)	0.2419 (3)	−2.659 (7)	2.604 (8)	3.193 (8)	2.8 (3)	4.4 (4)	5.6 (4)	4.8 (5)	4.8 (5)	3.0 (4)
Ring 4	0.3180 (3)	0.1703 (3)	0.2114 (4)	2.960 (20)	−1.909 (6)	−1.978 (20)	2.9 (3)	3.2 (4)	3.5 (4)	4.6 (4)	3.8 (4)	3.2 (3)
Ring 5	0.1527 (3)	0.1384 (4)	0.2502 (4)	0.890 (13)	−2.171 (7)	2.307 (13)	3.7 (4)	4.7 (5)	4.6 (4)	5.3 (5)	4.7 (4)	4.0 (4)
Ring 6	0.0043 (4)	0.2850 (4)	0.1509 (4)	−0.092 (7)	−3.139 (9)	−2.841 (8)	3.8 (4)	4.9 (4)	5.7 (5)	5.1 (5)	5.9 (5)	4.9 (4)
Ring 7	0.0388 (4)	0.2961 (4)	0.3784 (4)	−2.514 (11)	−2.335 (8)	0.395 (11)	3.3 (4)	3.9 (4)	4.9 (5)	6.1 (6)	4.9 (5)	4.0 (4)
Ring 8	0.1775 (4)	0.4615 (4)	0.4296 (4)	−1.854 (9)	−2.828 (8)	2.488 (9)	4.1 (4)	4.6 (4)	4.6 (4)	6.0 (6)	7.5 (8)	5.4 (5)

[a] The form of the thermal ellipsoid is $\exp[-(\beta_{11}h^2 + \beta_{22}k^2 + \beta_{33}l^2 + 2\beta_{12}hk + 2\beta_{13}hl + 2\beta_{23}kl)]$. [b] Standard deviations of the least significant figure(s) are given in parentheses. [c] C5, C6, and N comprise the acetonitrile molecule. [d] For definition of group parameters, see R. Eisenberg and J. A. Ibers, *Inorg. Chem.*, **4**, 773 (1965). [e] B_n is the temperature factor in Å^2 of atom Cn in the phenyl ring.

Table III. Derived Group Atom Positional Parameters

Atom	x	y	z	Atom	x	y	z
1C1[a]	0.2916 (5)	0.3778 (6)	0.0877 (6)	5C1	0.1495 (5)	0.1955 (4)	0.2221 (6)
1C2	0.3316 (7)	0.4216 (5)	0.1102 (6)	5C2	0.1750 (6)	0.1476 (6)	0.1883 (4)
1C3	0.3903 (6)	0.4242 (6)	0.0860 (7)	5C3	0.1783 (6)	0.0904 (5)	0.2163 (6)
1C4	0.4089 (5)	0.3830 (7)	0.0393 (7)	5C4	0.1560 (6)	0.0813 (4)	0.2782 (6)
1C5	0.3689 (7)	0.3392 (6)	0.0168 (6)	5C5	0.1304 (6)	0.1292 (6)	0.3121 (4)
1C6	0.3102 (6)	0.3366 (5)	0.0411 (6)	5C6	0.1272 (5)	0.1863 (5)	0.2841 (5)
2C1	0.1817 (6)	0.4506 (5)	0.0869 (6)	6C1	0.0642 (4)	0.2794 (6)	0.1707 (6)
2C2	0.1280 (6)	0.4494 (5)	0.0518 (7)	6C2	0.0293 (6)	0.2278 (4)	0.1606 (7)
2C3	0.1043 (5)	0.5029 (7)	0.0269 (6)	6C3	−0.0307 (6)	0.2334 (5)	0.1408 (7)
2C4	0.1343 (6)	0.5575 (5)	0.0370 (7)	6C4	−0.0556 (4)	0.2905 (6)	0.1311 (7)
2C5	0.1880 (6)	0.5586 (5)	0.0720 (7)	6C5	−0.0206 (6)	0.3421 (5)	0.1411 (6)
2C6	0.2117 (4)	0.5051 (6)	0.0970 (6)	6C6	0.0393 (6)	0.3365 (4)	0.1609 (6)
3C1	0.3589 (4)	0.3490 (5)	0.2449 (5)	7C1	0.0962 (4)	0.3161 (5)	0.3606 (6)
3C2	0.3646 (4)	0.4059 (5)	0.2731 (6)	7C2	0.0453 (6)	0.3367 (5)	0.3276 (5)
3C3	0.4196 (5)	0.4365 (4)	0.2701 (6)	7C3	−0.0120 (5)	0.3167 (6)	0.3454 (7)
3C4	0.4688 (4)	0.4103 (5)	0.2390 (6)	7C4	−0.0185 (4)	0.2762 (6)	0.3963 (7)
3C5	0.4631 (4)	0.3535 (6)	0.2107 (6)	7C5	0.0323 (6)	0.2556 (5)	0.4293 (6)
3C6	0.4081 (5)	0.3228 (4)	0.2137 (5)	7C6	0.0897 (5)	0.2755 (6)	0.4114 (6)
4C1	0.3033 (5)	0.2285 (3)	0.2318 (5)	8C1	0.1749 (6)	0.4102 (5)	0.3909 (6)
4C2	0.3139 (5)	0.2172 (4)	0.1669 (5)	8C2	0.1263 (5)	0.4504 (6)	0.3924 (6)
4C3	0.3286 (5)	0.1590 (5)	0.1465 (4)	8C3	0.1290 (5)	0.5017 (5)	0.4311 (6)
4C4	0.3326 (5)	0.1121 (4)	0.1910 (5)	8C4	0.1802 (7)	0.5129 (6)	0.4683 (6)
4C5	0.3220 (5)	0.1234 (4)	0.2560 (5)	8C5	0.2287 (5)	0.4727 (7)	0.4669 (6)
4C6	0.3074 (5)	0.1816 (5)	0.2764 (4)	8C6	0.2260 (5)	0.4214 (6)	0.4281 (7)

[a] 1C1 is C1(attached to P) of ring 1, etc.

7.0 Å^2 were used. The ensuing refinement yielded $R_1 = 0.058$ and $R_2 = 0.096$.

Comparison of the 103 observed Friedel pairs (hkl *vs.* $hk\bar{l}$) in the $1° \leq \theta \leq 15°$ shell indicated that the arbitrarily chosen enantiomorphic structure for this crystal was correct.

A final difference Fourier synthesis revealed three rather diffuse peaks (0.9–0.3 e/Å^3) positioned 3.3–5.8 Å from the chloride anion, whose linear arrangement seemed indicative of the acetonitrile of solvation. These positional parameters were included in the final least-squares cycle, but were not varied. Distance calculations indicate that the solvent molecule is positioned in a hole of more than sufficient size to accommodate it. Thus the high thermal motion on this molecule, as suggested by the ensuing refinement, is not surprising. It is important to note that no significant shifts in the coordinates of the other atoms resulted from the inclusion of the solvate molecule. The final values of R_1 and R_2 are 0.050 and 0.065, respectively.

Analysis of $|F_o|$ *vs.* $|F_c|$ for different classes of reflections, based on $|F_o|$, $\lambda^{-1} \sin \theta$, and even-odd combinations of indices failed to show any systematic trends. The error in an observation of unit weight is 2.21. The

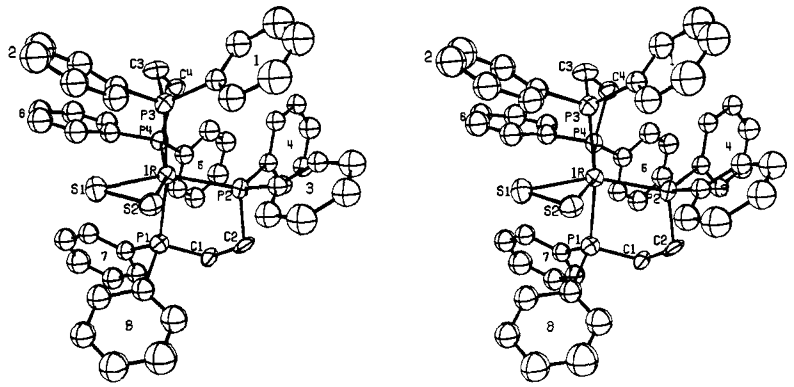

Figure 1. A drawing of the $[Ir(S_2)(dppe)_2]^+$ complex cation. The atoms are represented by 50% probability ellipsoids or spheres. Hydrogen atoms have been omitted for the sake of clarity. The two views constitute a stereoscopic pair that can be viewed with a small hand stereoscope.

observed and calculated amplitudes, $10|F_o|$ and $10|F_c|$, in electrons, are given in Table I.[24] Table II lists the final positional, thermal, and group parameters while Table III shows the derived positional parameters of the group atoms. Calculated hydrogen positional parameters are listed in Table IV. Table V presents the root-mean-square components of thermal vibration.

Table IV. Calculated Hydrogen Atom Parameters

Atom[a]	x	y	z	Atom	x	y	z
1H2[b]	0.318	0.451	0.143	5H6	0.108	0.220	0.308
1H3	0.419	0.455	0.102	6H2	0.047	0.186	0.167
1H4	0.451	0.384	0.021	6H3	−0.055	0.196	0.133
1H5	0.382	0.309	−0.016	6H4	−0.098	0.294	0.116
1H6	0.281	0.305	0.024	6H5	−0.038	0.383	0.134
2H2	0.106	0.410	0.044	6H6	0.064	0.373	0.168
2H3	0.065	0.502	0.001	7H2	0.050	0.365	0.291
2H4	0.117	0.595	0.019	7H3	−0.048	0.331	0.321
2H5	0.209	0.597	0.079	7H4	−0.059	0.261	0.409
2H6	0.250	0.506	0.122	7H5	0.027	0.226	0.465
3H2	0.325	0.422	0.296	7H6	0.126	0.260	0.435
3H3	0.418	0.477	0.291	8H2	0.089	0.442	0.365
3H4	0.504	0.434	0.236	8H3	0.094	0.530	0.432
3H5	0.496	0.337	0.187	8H4	0.182	0.549	0.496
3H6	0.403	0.282	0.192	8H5	0.265	0.480	0.493
4H2	0.311	0.250	0.134	8H6	0.260	0.392	0.427
4H3	0.336	0.150	0.099	H1[c]	0.321	0.271	0.361
4H4	0.343	0.070	0.176	H2	0.301	0.349	0.364
4H5	0.324	0.089	0.288	H3	0.212	0.243	0.354
4H6	0.299	0.189	0.323	H4	0.224	0.290	0.423
5H2	0.191	0.154	0.143	H5	0.221	0.240	0.104
5H3	0.196	0.055	0.191	H6	0.146	0.223	0.078
5H4	0.158	0.040	0.298	H7	0.124	0.330	0.064
5H5	0.114	0.122	0.356	H8	0.192	0.313	0.022

[a] All atoms were allotted values of $B = 7.0$ Å². [b] 1H2 is attached to C2 of ring 1, etc. [c] H1–H8 are attached to the aliphatic carbon atoms.

Description of the Structure

The $[Ir(S_2)(dppe)_2]Cl \cdot CH_3CN$ crystal structure consists of well-separated complex cations, the closest Ir–Ir contact being 10.5 Å. Approaches ranging upward from 2.36 Å occur between phenyl hydrogen atoms of adjacent complex units. Three chlorine-phenyl hydrogen atom distances (2.74–2.87 Å) are less than 3.0 Å. The acetonitrile molecules are arranged about the $\bar{4}$ axis at (0, 0, 0) with the $CH_3—C{\equiv}N$ methyl group directed toward the chloride anion (C5—C6···Cl, 149.6°; C6···Cl, 3.32 Å).

Table V. Root-Mean-Square Components of Thermal Displacement (Å) along Principal Axes

	Min	Intermed	Max
Ir	0.163 (2)	0.183 (2)	0.188 (1)
S1	0.194 (7)	0.211 (6)	0.255 (7)
S2	0.196 (7)	0.211 (7)	0.233 (6)
P1	0.183 (7)	0.192 (7)	0.208 (7)
P2	0.163 (7)	0.187 (7)	0.205 (7)
P3	0.181 (8)	0.193 (7)	0.208 (7)
P4	0.161 (8)	0.199 (7)	0.210 (7)
C1	0.15 (3)	0.22 (3)	0.22 (3)
C2	0.11 (4)	0.23 (2)	0.26 (2)
C3	0.18 (3)	0.19 (3)	0.27 (3)
C4	0.18 (3)	0.21 (3)	0.24 (3)
Cl	0.229 (7)	0.246 (7)	0.354 (7)

A stereoscopic view of the $[Ir(S_2)(dppe)_2]^+$ ion is shown in Figure 1, while the inner coordination sphere and chelate rings are displayed in Figure 2. Table VI provides selected interatomic distances and angles, together with their standard deviations as estimated from the correlation matrix. Despite differing space groups ($P\bar{4}2_1c$ *vs.* $P2_1/n$), anions (Cl^- *vs.* PF_6^-), and diatomic molecules (S_2 *vs.* O_2), the $[Ir(S_2)(dppe)_2]^+$ geometry is remarkably similar to those of $[M(O_2)(dppe)_2]^+$ (M = Ir, Rh) previously reported (Table VI) and is in accordance with Ginsberg and Lindsell's prediction.[14] All three ions may be described as trigonal-bipyramids with the group VIa diatomic molecule π bonded at equatorial positions. The two dppe rings span axial-equatorial edges to produce a cation with pseudo-C_2 symmetry. However, the longer 2.41 (2)-Å average Ir–S and 2.066 (6)-Å S–S distances in the disulfur complex make the distorted *cis*-octahedral assignment equally tenable.

The dppe Chelate Rings. In contrast to the $[Ir(O_2)(dppe)_2]^+$ complex (Table VII), Ir–P axial and equatorial bond lengths (Table VI) display a reasonable degree of consistency. Tabulations of iridium-phosphine distances compiled by others[25] imply no peculiarities in

[24] A listing of the structure factor amplitudes (Table I) will appear following these pages in the microfilm edition of this volume of the journal. Single copies may be obtained from the Business Operations Office, Books and Journals Division, American Chemical Society, 1155 Sixteenth St., N.W., Washington, D. C. 20036, by referring to code number JACS-72-3413. Remit check or money order for $4.00 for photocopy or $2.00 for microfiche.

[25] B. A. Frenz and J. A. Ibers, *Bien. Rev. Chem., Phys. Chem. Ser.*, in press,

Table VI. Intramolecular Bond Distances (Å) and Angles (deg)

		Iridium Coordination Sphere			
Ir-S1	2.422 (4)	S1-Ir-S2	50.8 (2)	S1-Ir-P1	84.6 (2)
Ir-S2	2.389 (5)	Ir-S1-S2	63.7 (2)	S1-Ir-P2	149.1 (2)
S1-S2	2.066 (6)	Ir-S2-S1	65.4 (2)	S1-Ir-P3	87.0 (2)
				S1-Ir-P4	111.9 (2)
Ir-P1(ax)	2.371 (5)	P1-Ir-P3	171.6 (2)	S2-Ir-P1	88.3 (2)
Ir-P2(eq)	2.331 (4)	P1-Ir-P4	98.7 (2)	S2-Ir-P2	99.8 (2)
Ir-P3(ax)	2.363 (5)	P2-Ir-P3	102.2 (2)	S2-Ir-P3	86.8 (1)
Ir-P4(eq)	2.337 (4)	P2-Ir-P4	98.5 (2)	S2-Ir-P4	160.9 (2)
		dppe Chelate Rings			
P1-C1	1.84 (2)	P1-Ir-P2	85.3 (2)	P3-Ir-P4	84.0 (2)
P2-C2	1.84 (2)	Ir-P1-C1	106.3 (6)	Ir-P3-C3	106.1 (6)
P3-C3	1.86 (2)	P1-C1-C2	106.6 (11)	P3-C3-C4	112.3 (13)
P4-C4	1.85 (2)	C1-C2-P2	110.8 (11)	C3-C4-P4	109.2 (13)
C1-C2	1.57 (2)	C2-P2-Ir	106.0 (6)	C4-P4-Ir	106.0 (6)
C3-C4	1.44 (2)	7C1-P1-8C1	99.7 (8)	1C1-P3-2C1	103.8 (8)
P1-7C1	1.82 (2)	7C1-P1-C1	104.5 (9)	1C1-P3-C3	105.3 (9)
P1-8C1	1.82 (2)	7C1-P1-Ir	120.2 (6)	1C1-P3-Ir	118.3 (6)
P2-3C1	1.84 (2)	8C1-P1-C1	105.4 (9)	2C1-P3-C3	104.2 (9)
P2-4C1	1.86 (2)	8C1-P1-Ir	119.1 (6)	2C1-P3-Ir	117.7 (6)
P3-1C1	1.84 (2)	3C1-P2-4C1	105.4 (8)	5C1-P4-6C1	102.1 (8)
P3-2C1	1.86 (2)	3C1-P2-C2	98.0 (8)	5C1-P4-C4	104.4 (8)
P4-5C1	1.82 (2)	3C1-P2-Ir	118.4 (6)	5C1-P4-Ir	124.2 (6)
P4-6C1	1.84 (2)	4C1-P2-C2	104.6 (8)	6C1-P4-C4	99.4 (8)
		4C1-P2-Ir	121.1 (6)	6C1-P4-Ir	117.4 (6)
		Acetonitrile Solvate Molecule[a]			
C5-C6	1.51	C5-N	1.15	C6-C5-N	180.0

[a] This geometry was assumed and was not varied.

the Ir-P bonding of $[Ir(S_2)(dppe)_2]^+$. Whether the shorter Ir-P_{eq} bonds result from an S_2-induced "trans" effect or valence-bond repulsions as predicted for d^8 five-coordinate complexes[26] is uncertain. Since trigonal-bipyramidal $[IrH(NO)(P(C_6H_5)_3)_3][ClO_4]$ has Ir-P_{eq} bond lengths of 2.334 (8), 2.341 (8), and 2.346 (9) Å,[27] S_2 complexation would seem to have little effect on Ir-P_{eq} bonding in the disulfur species.

The shorter 1.793-Å mean P-C_{phenyl} distance in $[Ir(O_2)(dppe)_2]^+$ is thought to be indicative of considerable electron flow into the O_2 molecule.[5] The mean P-C_{phenyl} bond length in the present compound of 1.838 Å is in better agreement with the corresponding value of 1.822 Å in $[Rh(O_2)(dppe)_2]^+$. These results are also in accord with the weaker electron acceptor properties of S_2. While the 1.85 (2)-Å average P-C_{ethyl} bond lengths are equivalent to those in other structures, one ethylenic C-C distance (1.44 (2) Å) is significantly shorter than the second (1.57 (2) Å).[28]

Both dppe chelate rings are puckered with 51.9 and 55.2° torsional angles about C1-C2 of the P1-C1-C2-P2 linkage and C3-C4 of the P3-C3-C4-P4 linkage, respectively. The dihedral angle formed by the Ir-P1-C1 and Ir-P2-C2 planes is 17.9 (6)°; the angle formed by Ir-P3-C3 and Ir-P4-C4 is a comparable 19.6 (6)°. Best least-squares planes (Table VIII) through the rings indicate that C3 and C4 of ring 2 are much less symmetrically disposed to the P3-Ir-P4 plane than are C1 and C2 in ring 1. The perspective depicted in Figure 2 as well as those given in ref 5 and 29 overemphasize this discrepancy.

The eight phenyl substituents in the disulfur complex exhibit a surprisingly regular arrangement not dissimilar to that found in the $[M(O_2)(dppe)_2]^+$ complexes. Six phenyl rings (1, 2, 4, 5, 7, and 8) are nearly parallel (average deviation 9.7°; Table IX) to the *n*C1-P*m*-C*m* plane. Phenyls 3 and 6, those closest to the S_2 molecule, display significantly larger dihedral angles (Table IX). The four rings (1, 2, 7, 8) attached to the apically coordinated phosphorus atoms seem capable of free rotation, but their particular orientations probably allow for a more compact molecule along the axial direction. Phenyls 4 and 5 are only 3.8 Å apart, and their planes are nearly parallel (dihedral angle, 14.9°). On the assumption that the P2-Ir-P4 angle is relatively inflexible and the van der Waal's half-thickness of a ben-

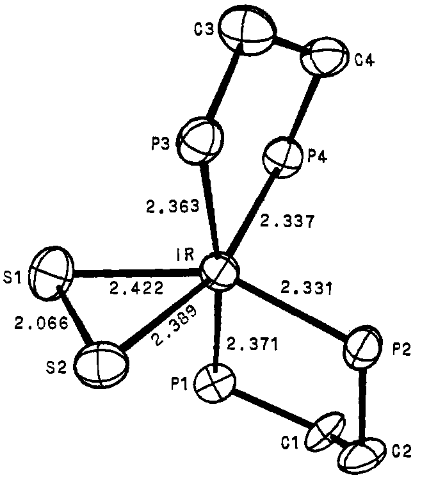

Figure 2. The $[Ir(S_2)(dppe)_2]^+$ inner coordination sphere and dppe chelate rings are depicted with 50% probability ellipsoids.

---

(26) R. J. Gillespie, *J. Chem. Soc.*, 4679 (1963).

(27) D. M. P. Mingos and J. A. Ibers, *Inorg. Chem.*, 10, 1479 (1971).

(28) The fact that other presumed equivalent distances in the molecule agree within limits consistent with the derived standard deviations leads us to conclude that these estimated standard deviations are reasonable. Thus, the two ethylenic C-C distances appear to differ significantly, but we can offer no explanation for this.

(29) C. G. Pierpont, A. Pucci, and R. Eisenberg, *J. Amer. Chem. Soc.*, 93, 3052 (1971).

Table VII. $[M(X)(dppe)_2]^+$ Polyhedral Parameters[a]

M	X	X-X′	M-X (X′)	X-M-X′	M-P(ax)	M-P(eq)	P(eq)-M-P(eq)′	P(eq)-M-X	P(eq)′-M-X′	Ref
Ir	CO		1.82 (2)		2.37 (2)	2.37 (2)	108 (1)	143 (2)	109 (2)	*b*
Ru	NO		1.735		2.408 2.377	2.357 2.410				*c*
Rh	O_2	1.418 (11)	2.026 (8) 2.025 (9)	41.0 (3)	2.362 (4) 2.354 (4)	2.326 (4) 2.350 (4)	98.1 (1)	108.9 (3)	113.0 (3)	5
Ir	O_2	1.625 (23)	1.961 (18) 1.990 (16)	48.6 (7)	2.349 (7) 2.336 (7)	2.283 (7) 2.452 (9)	96.0 (3)	105.4 (6)	111.1 (5)	5
Ir	S_2	2.066 (6)	2.422 (4) 2.389 (5)	50.8 (2)	2.371 (5) 2.363 (5)	2.331 (4) 2.337 (4)	98.5 (2)	99.8 (2)	111.9 (2)	This work

[a] X occupies a trigonal-bipyramidal equatorial position. Bond lengths are in angströms; angles are in degrees. [b] J. A. J. Jarvis, R. H. B. Mais, P. G. Owston, and K. A. Taylor, *Chem. Commun.*, 906 (1966). [c] C. G. Pierpont, A. Pucci, and R. Eisenberg, *J. Amer. Chem. Soc.*, **93**, 3052 (1971).

Table VIII. Weighted Least-Squares Planes

Atom	Equatorial[a] Distance, Å	Atom	Chelate ring 1[b] Distance, Å	Atom	Chelate ring 2[c] Distance, Å
Ir	−0.0016 (7)	Ir	−0.0006 (6)	Ir	0.0006 (7)
S1	−0.206 (5)	P1	0.022 (5)	P3	−0.012 (5)
S2	0.151 (4)	P2	−0.008 (4)	P4	−0.031 (4)
P2	−0.082 (4)	C1	−0.45 (2)	C3	−0.12 (2)
P4	0.099 (5)	C2	0.34 (2)	C4	0.56 (2)

[a] For $7.230x + 3.769y - 19.280z = -1.632$. x, y, and z are fractional coordinates. [b] For $8.933x + 19.664y + 4.279z = +9.723$. [c] For $18.904x - 11.379y + 0.557z = -0.194$.

Table IX. Dihedral Angle between Planes

Plane I	Plane II	Dihedral angle, deg
Axial Diphenylphosphine Groups		
P1-C1-7C1	Phenyl 7	18.5
P1-C1-8C1	Phenyl 8	22.6
P3-C3-1C1	Phenyl 1	5.3
P3-C3-2C1	Phenyl 2	16.4
Equatorial Diphenylphosphine Groups		
P2-C2-3C1	Phenyl 3	68.0
P2-C2-4C1	Phenyl 4	8.7
P4-C4-5C1	Phenyl 5	5.8
P4-C4-6C1	Phenyl 6	81.0
Interphenyl Angles		
Phenyl 4	Phenyl 5	14.9
Phenyl 3	Phenyl 4	72.5
Phenyl 5	Phenyl 6	84.1

zene ring is 1.70 Å,[30] one would expect rotation about the P4-5C1 and the P2-4C1 bonds to be restricted.

The calculated positions of 3H2 and 6H6 are 2.57 and 2.54 Å from S2 and S1, respectively. The 3C2—3H2···S2 and 6C6—6H6···S1 angles are 130.7 and 155.4°. A covalent interaction may be operative, involving the phenyl hydrogen atoms and the metal-electron enriched $p\pi^*$ sulfur orbitals. In fact, the distorted $[Ir(CO)(dppe)_2]^+$ structure has been rationalized in terms of Ir-H bonding between the metal and phenyl ortho hydrogen atoms.[31]

Iridium-Disulfur Bonding. A study of Figure 2 and Table VI indicates that the IrS_2P_4 coordination polyhedron deviates significantly from any idealized geometrical form. The S_2 molecule is twisted 12.8 (2)° out of the P2-Ir-P4 equatorial plane toward those polyhedral edges not spanned by the dppe chelate rings. This distortion may reflect P-C-C-P ring constraints; however, ligand-ligand repulsion forces would also seem to favor this arrangement. The two iridium-sulfur distances of 2.422 (4) and 2.389 (5) Å differ by more than 6σ, as do the S-Ir-P angles (111.9 (2), 99.8 (3)°) in the polyhedral equatorial plane. Other structures (Table VII) reflect similar distortions.

The Ir-S bond lengths lie between the 2.24-Å iridium-sulfur distances of the octahedral iridium(III) complex, $[IrCl_2(C_{15}H_{13}O)((CH_3)_2SO)_2]$,[32] and the longer 2.49 (1)-Å Ir-S bond in five-coordinate $[IrCl(SO_2)(CO)(P(C_6H_5)_3)_2]$.[33] McPartlin and Mason[32] have estimated the sum of Ir(III)-S covalent radii at 2.43 Å, slightly more than the 2.41 (3)-Å average Ir-S lengths in $[Ir(S_2)(dppe)_2]^+$. But changes in metal coordination number and charge as well as the variability of substituents attached to sulfur preclude a more detailed comparison.

As observed for molecular oxygen in the $[IrX(O_2)(CO)(P(C_6H_5)_3)_2]$ and $[M(O_2)(dppe)_2]^+$ cations, disulfur exhibits S-S bond lengthening on complexation to iridium. The 2.066 (6)-Å disulfur bond in $[Ir(S_2)(dppe)_2]^+$ is approximately that in octasulfur, 2.060 (3);[34] H_2S_2, 2.06 (2);[35] phenyl disulfide, 2.03 (1);[36] and in $[SFe(CO)_3]_2$, 2.007 (5) Å, where an S_2 group bridges two $Fe(CO)_3$ groups.[37] It is somewhat shorter than the 2.15- and 2.13-Å S-S bond lengths in the BaS_3[38] and Na_2S_2[39] salts, respectively. More striking is the contrast provided by $[NbCl(Cp)_2(S_2)]$,[13] where the π-bonded disulfur molecule displays a 1.73-Å S≡S triple bond.

Metal-oxygen bonding in the d^8 molecular oxygen carriers has been discussed in terms of the Chatt-Dewar model.[8,9] A σ bond is formed by $\pi(O_2) \rightarrow d(M)$ donation from the filled O_2 π level into an empty d-type metal orbital. Back-bonding then occurs into the ligand π^* orbital, thereby reducing the $L(\delta^+) \rightarrow M(\delta^-)$ dipole. Thus O-O bond lengths have been correlated with the availability of metal d-electron density for back-donation into the in-plane O_2 π^* orbital.[3-5] Attachment of

---

(30) L. Pauling, "The Nature of the Chemical Bond," 3rd ed, Cornell University Press, Ithaca, N. Y., 1960, p 260.

(31) J. A. J. Jarvis, R. H. B. Mais, P. G. Owston, and K. A. Taylor, *Chem. Commun.*, 906 (1966).

(32) M. McPartlin and R. Mason, *ibid.*, 545 (1967).

(33) S. J. La Placa and J. A. Ibers, *Inorg. Chem.*, **5**, 405 (1966).

(34) A. Caron and J. Donohue, *Acta Crystallogr.*, **18**, 562 (1965).

(35) M. K. Wilson and R. M. Badger, *J. Chem. Phys.*, **17**, 1232 (1949).

(36) J. D. Lee and M. W. B. Bryant, *Acta Crystallogr., Sect. B*, **25**, 2094 (1969).

(37) C. H. Wei and L. F. Dahl, *Inorg. Chem.*, **4**, 1 (1965).

(38) W. S. Miller and A. J. King, *Z. Kristallogr., Kristallgeometrie, Kristallphys., Kristallchem.*, **94**, 439 (1936).

(39) V. H. Föppl, E. Busmann, and F. K. Frorath, *Z. Anorg. Allg. Chem.*, **314**, 12 (1962).

less electronegative substituents (P < I < Cl) to the metal or reduction in metal d-orbital energies (Ir < Rh), results in longer O-O bonds, lower O-O bond orders, and stronger $M-O_2$ binding.

An identical bonding scheme can be applied to structures containing the less electronegative S_2 molecule. Sulfur-iridium $p\pi(S_2) \rightarrow d\ (Ir)\ \sigma$ bonding is complemented by $d\pi(Ir) \rightarrow p\pi^*(S_2)$ back-donation. Using the 1.889-Å S-S length[12] in disulfur (bond order 2) and the $S_2{}^{2-}$ distance of 2.12 Å in Na_2S_2[39] (bond order 1) as rough guides, the sulfur-sulfur distance of 2.066 (6) Å in $[Ir(S_2)(dppe)_2]^+$ corresponds to somewhat more than a single bond. On the other hand, the 1.625 (23)-Å O_2 bond in $[Ir(O_2)(dppe)_2]^+$ is 0.13 Å longer than the peroxo linkage in Na_2O_2,[40] suggesting an O-O bond order significantly less than one. As might have been predicted from simple electronegativity considerations, $\pi^*(O_2)$ is a better electron acceptor than $\pi^*(S_2)$.

Unlike oxygen, sulfur has lower lying d-type orbitals that have been invoked in the explanation of certain artifacts of sulfur chemistry.[11] If these orbitals do accept $d\pi(Ir) \rightarrow d\pi(S_2)$ electron density, Ir-S and S-S bonds might display more multiple-bond character. But the lower effective nuclear charge on the $[Ir(S_2)(dppe)_2]^+$ sulfur atoms, resulting from the lack of more electronegative substituents plus iridium-to-sulfur electron flow, implies little $d\pi(Ir) \rightarrow d\pi(S)$ interaction.

The short, 1.73-Å disulfur linkage in $[NbCl(Cp)_2(S_2)]$ reflects the drastic difference in $Nb(III)-S_2$ and $Ir(I)-S_2$ bonding. The electron-poor, d^2 niobium(III) ion evidently stabilizes S_2 *via* $p\pi^*(S_2) \rightarrow d\pi(Nb)$ *forward* π donation of the same type postulated in most earlier metal halide or chalconide complexes. Since this represents a reversal in π-electron flow, opposing secondary effects might also be expected.

Ginsberg and Lindsell[14] have indicated that S_2 is not displaced when O_2 is bubbled through an $[Ir(S_2)(dppe)_2]Cl$ solution for 12 hr. We therefore conclude that the $Ir-S_2$ bond lengths and angles cited herein correspond to those belonging to an irreversible disulfur carrier. To provide the background for a more quantitative analysis, it is clearly necessary to obtain additional structural data on closely related disulfur and diselenium complexes.

Acknowledgments. We are indebted to Dr. A. P. Ginsberg for supplying crystals as well as pertinent chemical information in advance of publication. Support of this work by the National Institutes of Health is gratefully acknowledged.

---

(40) R. L. Tallman, J. L. Margrave, and S. W. Bailey, *J. Amer. Chem. Soc.*, **79**, 2979 (1957).

Oxygen-17 Nuclear Magnetic Resonance Studies of Aqueous Nickel Ion

James W. Neely and Robert E. Connick*

Contribution from the Department of Chemistry, University of California, and the Inorganic Materials Research Division, Lawrence Radiation Laboratory, Berkeley, California 94720. *Received August 14, 1971*

Abstract: In aqueous solutions of nickelous ion, the bulk water nmr line widths of oxygen-17 have been measured from about 0 to 150° at 2.00 and 8.134 MHz. The chemical shift of bulk water oxygen was similarly measured at 8.143 MHz. The ^{17}O nmr spectrum of water in the first coordination sphere of Ni^{2+} ion has been reexamined under more favorable experimental conditions. The results of these studies are consistent with six equivalent waters composing the first coordination sphere of Ni^{2+} over the temperature range covered. The enthalpy and entropy of activation for water exchange has been calculated to be 13.9 kcal/mol and 10 eu, respectively, with a scalar coupling constant (A/h) to the ^{17}O of $2.4 \times 10^{+7}$ Hz. In agreement with the results of Fiat, a small residual chemical shift of ^{17}O of bulk water was observed at low temperature. It is concluded that the shift must be attributed to second coordination sphere interactions. The experimental frequency dependence of the relaxation of ^{17}O caused by scalar coupling has been used to calculate a correlation time for the electronic relaxation of Ni^{2+} of 1.1×10^{-12} sec at 160°. In the low-frequency limit at 2.00 MHz, the electronic relaxation times, T_{1e} and T_{2e}, are found to be 5.8×10^{-12} sec at 160°, with an activation energy of 1.2 kcal/mol. Another independent measure of the electronic relaxation correlation time has been obtained by extending the work of Morgan and Nolle on protons to 220 MHz. The apparent lack of a dispersion region in the frequency dependence of the dipolar coupling to the protons has been shown to be due to a competing frequency dependence of the electronic relaxation. An electronic correlation time of 1.0×10^{-12} is consistent with these data as well.

The first hydration sphere of nickelous ion in aqueous solution has been studied in the past by ^{17}O nmr.[1-4] The results of these studies have led to some perplexing contradictions which have cast doubt on the previous chemical knowledge of the Ni^{2+} ion or on the adequacy of the general exchange theory governing nmr line widths. From proton nuclear magnetic resonance measurements near −30° in concentrated aqueous salt so-

---

(1) T. J. Swift and R. E. Connick, *J. Chem. Phys.*, **37**, 307 (1962); **41**, 2553 (1964).

(2) R. E. Connick and D. Fiat, *ibid.*, **44**, 4103 (1966).

(3) D. Fiat in "Magnetic and Electric Resonance and Relaxation," North Holland Publishing Co., Amsterdam, 1967.

(4) A. G. Desai, H. W. Dodgen, and J. P. Hunt, *J. Amer. Chem. Soc.*, **92**, 798 (1970).